IEEE Access
Multidisciplinary | Rapid Review | Open Access Journal

Received July 14, 2021, accepted July 25, 2021, date of publication July 28, 2021, date of current version August 5, 2021.

*Digital Object Identifier 10.1109/ACCESS.2021.3100995*

# Dual MIMO Antenna System for 5G Mobile Phones, 5.2 GHz WLAN, 5.5 GHz WiMAX and 5.8/6 GHz WiFi Applications

**PHALGUNI MATHUR[1], (Student Member, IEEE), ROBIN AUGUSTINE[2], (Member, IEEE), M. GOPIKRISHNA[3], (Member, IEEE), AND SUJITH RAMAN[1], (Senior Member, IEEE)**

[1]Department of Electronics and Instrumentation, Bharathiar University, Coimbatore, Tamil Nadu 641046, India
[2]Microwaves in Medical Engineering Group, Uppsala University, 75121 Uppsala, Sweden
[3]Department of Physics, Government Victoria College, Palakkad, Kerala 678001, India

Corresponding authors: Sujith Raman (sujithrpkd@gmail.com) and Robin Augustine (robin.augustine@angstrom.uu.se)

This work was supported by the University Grants Commission (UGC) of the Government of India through the Faculty Recharge Program. The work of Robin Augustine was supported in part by the Swedish SSF Project LifeSec under Grant RIT170020, and in part by the Project ZeroIoT under Grant CH10-0003.

**ABSTRACT** A multi-purpose dual Multiple-Input-Multiple-Output (MIMO) antenna system for 5G mobile systems is presented in this paper. The proposed antenna consists of two sets of MIMO antennas on a single board. The 8-port MIMO antenna, placed on the board, is working over 3.5 GHz (3.4 GHz-3.6 GHz) 5G band with dimensions 150 mm $\times$ 70 mm. The 4-port MIMO system, placed on the chassis, is operating over 5.2 GHz WLAN/5.5 GHz WiMAX/5.8 GHz/6 GHz WiFi band with dimensions 20 mm $\times$ 7 mm. The prototype is designed and fabricated on FR4 ($\epsilon_r = 4.4$ and $\tan\delta = 0.02$) substrate with 0.8 mm thickness. The overall design of the entire dual MIMO system is very minimal leaving ample space for other components to be placed on the board. The presence of two separate MIMO antennas in the proposed prototype aids in using the 5G frequencies and 4G frequencies independently. Since no active elements like diodes, switches etc. are involved in the proposed design to switch between different bands, the prototype is free from any ohmic losses. It is also worth noticing that the proposed antenna operates in the highly anticipated next generation WiFi 6E spectrum.

**INDEX TERMS** MIMO, WLAN, WiFi 6E, 5G mobile phones.

## I. INTRODUCTION

Communication has played a vital role in the evolution of mankind. The mode of communication between human beings has been subjected to constant development and improvement since the beginning of mankind. A few centuries ago, weather, word of mouth, line of sight etc. played a crucial role in the content and the quality of information transfer over long distances. However, since the paradigm shifting invention of electrical circuits and eventually the telegraph system in the 19th century, communication has become much more reliable, faster and efficient. In fact, when Maxwell's equations came to light, communication technology took an astronomical leap as it paved the way for wireless media to carry the information from one place to another as demonstrated by Heinrich Hertz in the late 1880's [1]. J.C. Bose's and G. Marconi's antennas further cemented the promising scope of wireless communication. Since then wireless communication technology has been constantly growing and evolving [2], [3].

One of the main components of a communication system is the antenna through which the information is transmitted/received to/through free space. In late 1980's, Winters proposed in [4] that if antenna arrays are used in a communication system, then, a method of spatial processing can be used to differentiate the uplink signals from different users [5]. In [6], the multipath channels associated with a communication system was exploited for their spatial properties. The authors theoretically demonstrated that the use of antenna arrays in a communication system specifically in a CDMA could greatly enhance its efficiency. These studies laid the foundation for multiple-input-multiple-output (MIMO) antenna systems. Modern communication systems make use of such systems that incorporate multiple

The associate editor coordinating the review of this manuscript and approving it for publication was Mahmoud A. Abdalla.

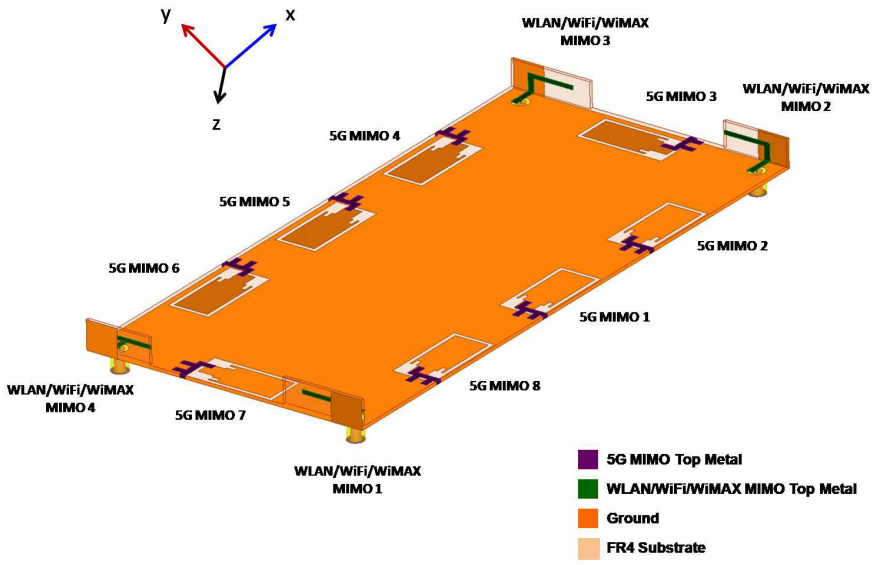


**FIGURE 1.** Dual MIMO antenna system consisting of an 8-port MIMO for 3.5 GHz 5G band and 4-port MIMO for WLAN/WiFi/WiMAX bands.

transmitter and receiver antennas to improve the overall efficiency of the system. The first practical demonstration of a MIMO system is presented in [7] where equal number of antenna array elements are employed at the transmitting and the receiving ends. This technology is fast growing in the telecom industry, taking just about a decade from conceptualization to wide spread application [8]. MIMO systems are extensively used in 4G LTE systems [9] and are anticipated to be included liberally in 5G systems as well.

In 5G systems, Massive MIMO with a large number of transmit and receive antennas are expected to play the lead role as they can provide higher data rates and increased channel capacities [10]. As the 5G technology is flourishing, scientists and engineers face the challenge to fit several antennas in a limited form factor with good isolation. A plausible solution is to use antennas operating in mm-wave frequencies 24 GHz, 28 GHz, 37 GHz, 39 GHz and 60 GHz included in the 5G spectrum [11]. It has been observed that for handheld devices, the path losses resulting from such antennas cannot be ignored [12]- [16]. Thus, phased array antennas are used to compensate for these losses. However, it is difficult to place a mm-wave antenna close to a 4G antenna due to the huge difference between the operating frequencies. In order to overcome that, 3.5 GHz band has been licensed for 5G technology. However, the amount of literature available for MIMO antennas working in 3.5 GHz band is fairly less when compared with mm-wave antennas. In [17], the authors presented a quad antenna system for cell phones, consisting of a dual port MIMO operating over the frequency range of 1.4 GHz to 3.7 GHz in conjunction with two other antennas working on other different bands. In [18] a quad-port MIMO antenna operating at 3.5 GHz 5G band is proposed. In [19] a dual port MIMO is proposed that could be used for 3.5 GHz mobile phone applications. In [20], two different configurations of 8-port MIMO are discussed for 3.5 GHz band.

In this paper, we propose a dual-MIMO system where a 8-port MIMO antenna system operating at 3.5 GHz frequency band is integrated with a 4-port multiband MIMO antenna system operating in the frequency range from 4.86 GHz to 6.93 GHz covering 5.2 GHz WLAN, 5.5 GHz WiMAX, 5.8 GHz WiFi and three channels of 6 GHz WiFi bands. To the best of authors' knowledge, this kind of multi MIMO system for 5G mobile antennas has not be reported yet. The 8-port MIMO system is designed and fabricated on FR4 substrate ($\epsilon_r = 4.4$ and $\tan\delta = 0.02$) with dimensions 150mm $\times$ 70 mm $\times$ 0.8 mm. The 4-port MIMO system is placed on the chassis with height 7 mm from the ground of the primary board. There are numerous merits of the proposed dual MIMO system. Firstly, the prototype contains two different sets of MIMO antenna systems working on two different frequency bands. It can be argued that a single frequency reconfigurable MIMO antenna would also help in switching the operating frequency bands. While this is true, it should be noted that such a reconfigurable antenna would make use of some kind of switching mechanisms like diodes, liquid crystals, motors, dielectric strips [21] etc. The addition of these components adds to the associated losses, payload and other complexities that reduce the overall efficiency of the entire system. With the proposed design such degradation can be avoided. Secondly, all radiating elements are sufficiently compact. Thirdly, the 4-port MIMO antenna covers the frequency band of highly anticipated 6 GHz WiFi band [22].

## II. ANTENNA DESIGN AND ANALYSIS

The schematic of the proposed dual MIMO system is shown in Fig. 1. For better description, this section presents the design evolution in two subsections. The first subsection

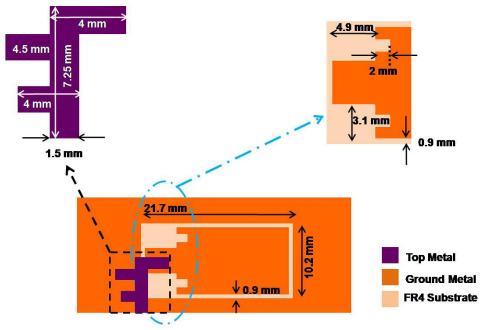


**FIGURE 2.** Single antenna element of 8-port MIMO antenna system.

deals with 8-port MIMO design evolution while the second subsection deals with 4-port MIMO. ANSYS HFSS was used to perform the entire modeling, parametric analysis and optimization.

### A. 8-PORT MIMO ANTENNA SYSTEM

The geometry of the single element of 8-port MIMO antenna system for 3.5 GHz is shown in Fig. 2. It consists of a folded transmission line feeding a rectangular loop of perimeter $1.2\lambda_g$ with dimensions $0.41\lambda_g \times 0.1\lambda_g$ etched on the ground of the FR4 substrate. From Fig. 3a, it is evident that by varying the length of the fold of the transmission line alone, desirable resonance and bandwidth cannot be achieved. For cases where a=2 mm and a=2.5 mm, it could be argued that by modifying the size of the rectangular loop the required bandwidth can be achieved. However, in order to do so it would be required to increase the length of the rectangular loop that could compromise the compactness as well as performance of the entire antenna. It is also seen from Fig. 4 that the nature of impedance for the loop antenna fed by the folded transmission line alone is significantly inductive. In order to address this issue, a capacitive stub (Stub1) is added to the folded transmission line. While Stub1 does help in decreasing the inductance, desired bandwidth and impedance matching is not achieved, as is evident from Fig. 5. In fact, the addition of Stub1 to the transmission line yields the bandwidth from 3.43 GHz to 3.66 GHz (230 MHz) exhibiting weak impedance matching with return loss of -15.28 dB at of 3.54 GHz. However, when a shorter capacitive stub (Stub2) is added to the folded transmission line, it is seen from Smith chart, that the inductance is greatly reduced and the resistance of the antenna element is increased. Specifically, Stub2 yields a bandwidth of 190 MHz ranging from 3.35 GHz to 3.54 GHz with a return loss of -12.21 dB at the resonant frequency 3.45 GHz. When these stubs are added simultaneously to the folded transmission line, a near perfect resonance at 3.5 GHz with operating band ranging from 3.37 GHz to 3.6 GHz is achieved, as shown in Fig. 4 and Fig. 5. The design of the rectangular loop is presented in three cases as shown in Fig. 3b. In the first case a simple rectangular loop of dimension $0.5\lambda_g \times 0.1\lambda_g$ was considered. The reflection coefficient obtained from this loop is shown

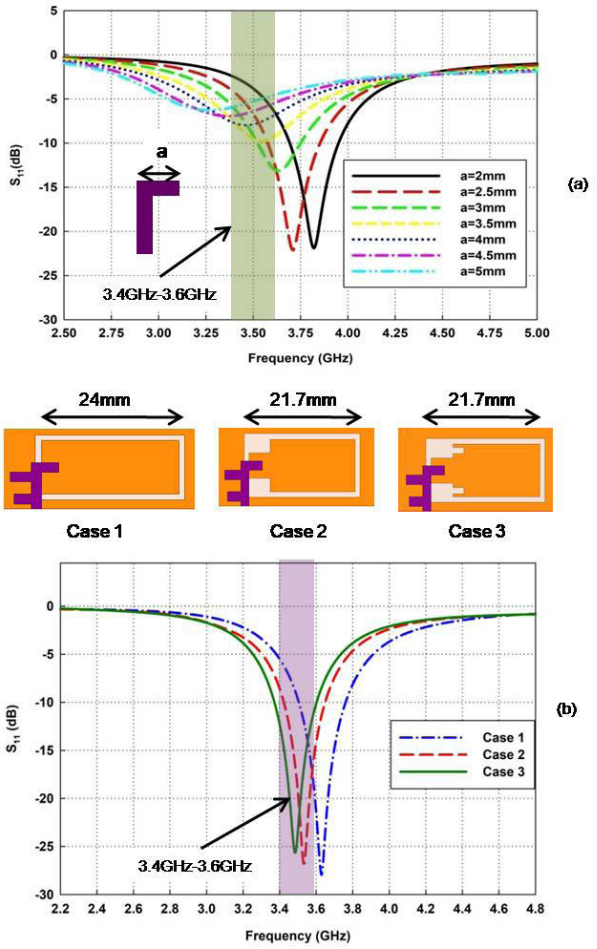


**FIGURE 3.** Design evolution of antenna element (a) Impedance characteristics observed by varying the length of the fold on the transmission line alone (b) Impedance characteristics observed during the evolution of the rectangular loop.

as Case 1 in Fig. 3b. The loop was operating within the frequency range of 3.5-3.75 GHz with resonant frequency at 3.62 GHz. In order to make the loop operate at a lower frequency band (3.5 GHz 5G band), either the dimensions of the loop could have been increased or additional slots could have been introduced within the loop geometry. Since physical compactness of the antenna element is preferred, two slots were introduced in the geometry while the overall dimension of the slot itself was optimized and reduced to $0.41\lambda_g \times 0.1\lambda_g$. The reflection coefficient obtained by adding the two slots is shown as Case 2 in Fig. 3b. The rectangular loop with two slots was operating within the frequency range of 3.45-3.65 GHz with operating frequency at 3.55 GHz. Two additional and smaller slots were placed as shown in Case 3 in Fig. 3b. Finally in this case, the loop was able to accommodate the entire 3.5 GHz band while operating within the frequency range of 3.37-3.6 GHz.

Along the longer edge of the board, the radiators are placed linearly at a distance of more than $\lambda_g/2$ between subsequent radiating elements to avoid higher mutual coupling.

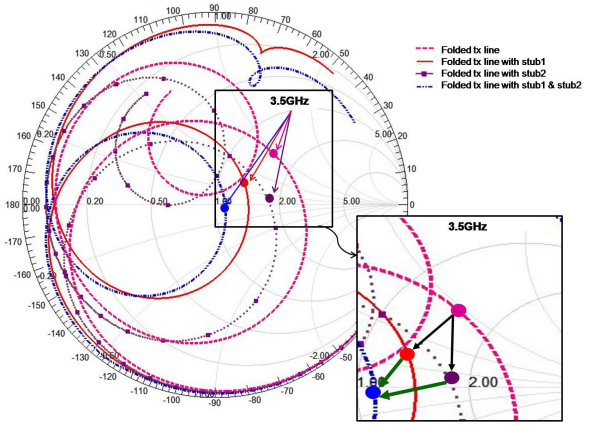


**FIGURE 4.** Effect of the two stubs on folded transmission line as seen on the Smith Chart.

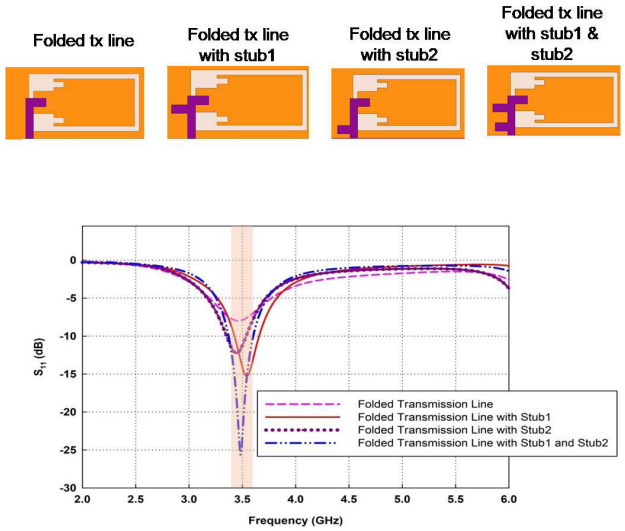


**FIGURE 5.** S-parameter analysis of the effect of two stubs on the folded transmission line.

The centers of MIMO antenna 1 (Ant1) and Ant5 are aligned with the center of the longer edge. Along the shorter edge of the board a single element is placed as shown in Fig. 1. The center of the slot is aligned with the center of the shorter edge. The fabricated prototype used for testing, is shown in Fig. 6.

The simulated and measured reflection coefficients of all the antenna elements for 8-port MIMO are shown in Fig. 7a and Fig. 7b respectively. It is evident that all the antenna elements individually cover the entire 3.5 GHz band. The measured results show a slight decrease in the impedance matching. This could be due to factors like cable losses, imperfect connections in the measurement setup etc. Even then, a good agreement between the simulated and the measured results is obtained. Fig. 7c and Fig. 7d depict the transmission coefficients between Ant1 and the rest of the radiating elements. Since Ant1 is in the immediate vicinity of Ant2 and Ant8, it shows least isolation with the two aforementioned radiators. To further support this argument,

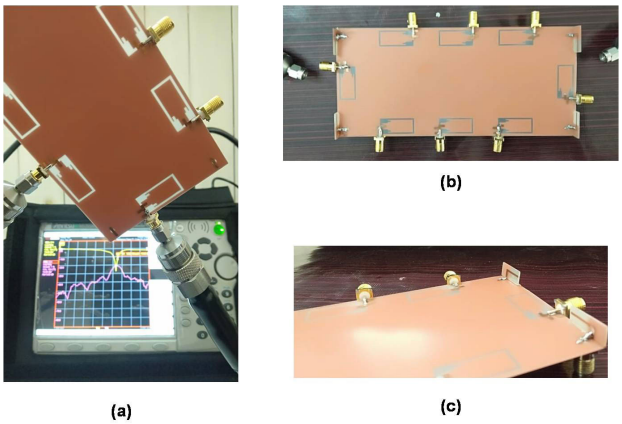


**FIGURE 6.** Fabricated prototype of the proposed dual MIMO antenna system.

the current distribution when only Ant1 is radiating and rest of the antenna inputs are terminated with 50Ω is shown in Fig. 8. It can be seen that when Ant1 is excited, it has maximum influence on Ant8 and Ant2 due to their mutual placement on the board. Even in this case, it is evident from Fig. 7c and Fig. 7d, that this effect of Ant1 on Ant 2 and Ant8 is less than generally accepted limits. Similar behavior was observed for Ant5, Ant4 and Ant6. The slight discrepancy in the measurement of some transmission coefficients is most likely due to fabrication and soldering errors. Even then all of the measured transmission coefficients lie within acceptable limits.

The radiation pattern of the individual elements of 8-port MIMO antenna is shown in Fig. 9. It is evident from the figure that despite having identical geometries, the radiation patterns of each element are not identical. This can be attributed to the placement of each radiator on the main board. Fig. 10 shows the exclusive current distribution of Ant1, Ant2, Ant3 and Ant8 in the absence of other radiators. While the radiating elements are placed symmetrically along the edges of the main board, the geometry of each antenna element are not symmetric. Hence, the current distribution of each antenna element is significantly different at different positions as shown in Fig. 10. This is also the reason that the radiation patterns of all elements of 8-port MIMO antenna have slightly varying radiation patterns. The gains obtained for the individual antenna elements for this MIMO ranges from 2.61 dB to 3.51 dB at 3.5 GHz. The Envelope Correlation Coefficient (ECC) is one of the most significant parameters of MIMO antennas. ECC is used to quantify the relation between the radiation characteristics of individual radiating elements of MIMO antenna. In this work, ECC is calculated using the far-field radiation patterns of individual antenna elements and was obtained using the equation [24]:

$$ECC = \frac{\int\int_{4\pi} Q_1 \cdot Q_2^* d\Omega}{\sqrt{\int\int_{4\pi} Q_1 Q_1^* d\Omega \cdot \int\int_{4\pi} Q_2 Q_2^* d\Omega}} \quad (1)$$

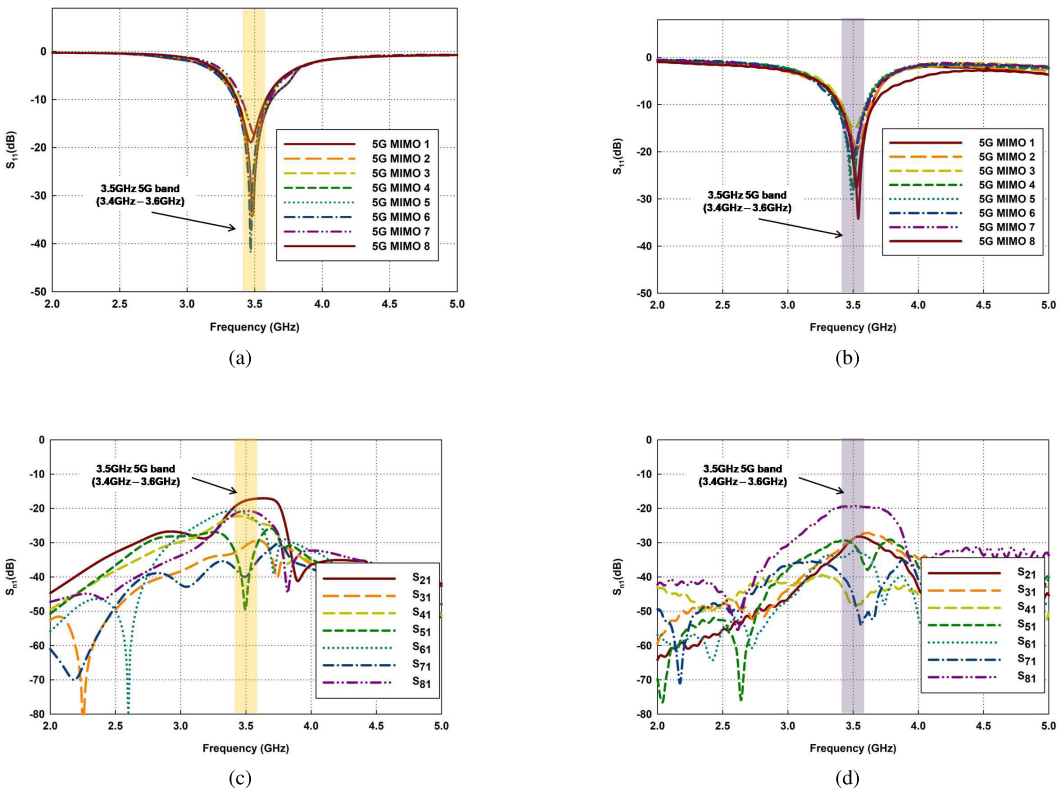


**FIGURE 7.** (a) Simulated reflection coefficients of individual radiating elements (b) Measured reflection coefficient of individual radiating elements (c) Simulated transmission coefficients between MIMO 1 and rest of the radiating elements (d) Measured transmission coefficients between MIMO 1 and rest of the radiating elements of 8-port 3.5 GHz MIMO antenna system.

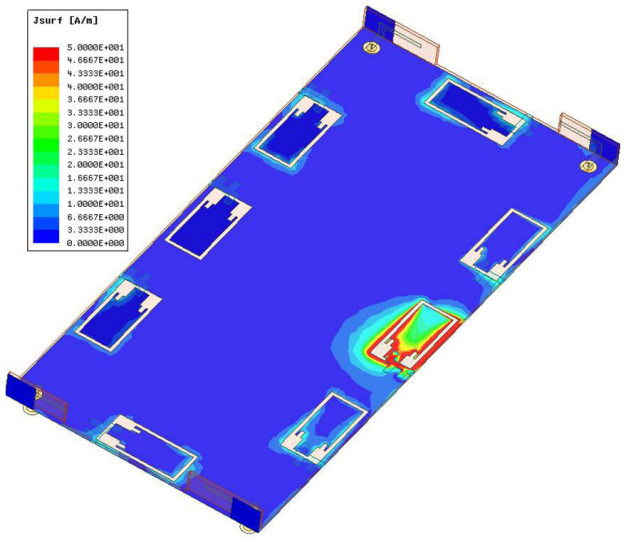


**FIGURE 8.** Current distribution when only MIMO antenna 1 is excited.

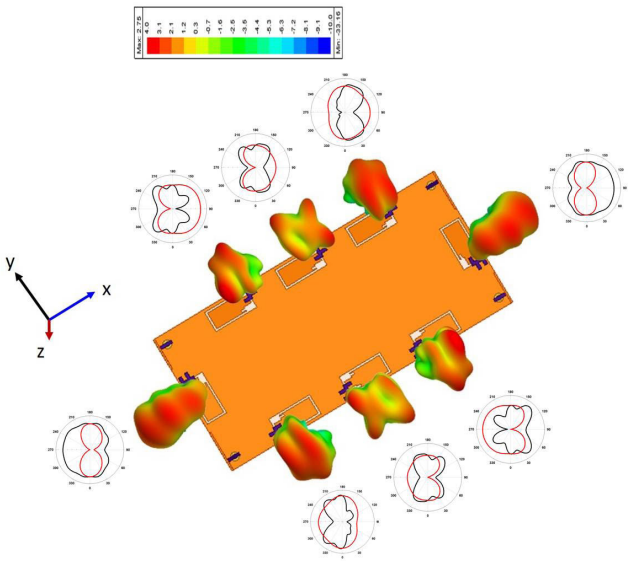


**FIGURE 9.** Radiation pattern for all antenna elements of 8-port 3.5 GHz MIMO.

where $Q_n$ is the far-field radiation pattern of the $n^{th}$ antenna. Fig 11 shows the ECC of Ant1 with respect to the rest of the antenna elements. The ECC for all the combinations was found to be less than 0.08 which is well within the accepted limits. Similar characteristics were observed for rest of the radiating elements of the proposed 8-port MIMO antenna.

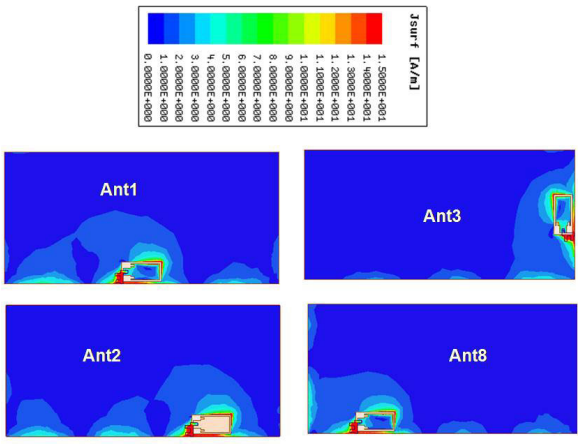


**FIGURE 10.** Individual current distributions of Ant1, Ant2, Ant3 and Ant8 in the absence of other radiators at 3.5GHz.

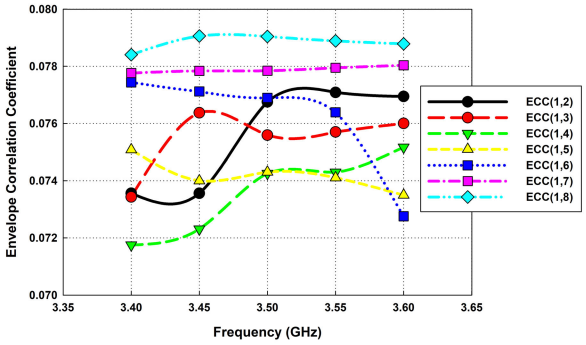


**FIGURE 11.** Envelope correlation coefficient between Ant1 and the rest of the radiating elements.

### *B. 4-PORT MIMO ANTENNA SYSTEM*

While the main board is occupied by the 5G MIMO antenna, the chassis of the proposed mobile phone antenna system houses a 4-port multiband MIMO antenna. The schematic of the single element of the proposed MIMO is shown in Fig. 12. Here, a double folded monopole antenna is used as the radiating element. The monopole is fed in the *xy*-plane using a probe feed, shown in blue. The feeding strip is then folded to *yz*-plane and continues along a truncated ground plane of dimensions 7.8mm $\times$ 7mm. Within the *yz*-plane, the monopole is turned again by 90° and extends beyond the truncated ground for about a quarter of the guided wavelength.

The radiation pattern of the individual radiating elements of multiband 4-port MIMO antenna system is shown in Fig. 13. The respective gain of each of the radiating element ranges from 4.99 dB to 5.33 dB at 5.2 GHz. Fig. 14 shows the impedance characteristics of multiband 4-port MIMO antenna system. Here we can see that all the antenna elements individually cover a broad frequency range from 5.02 GHz to 6.93 GHz. This frequency range makes the proposed MIMO system suitable for applications in the IEEE 802.11 bands i.e., 5.2 GHz WLAN band (5.15 GHz to 5.35 GHz) [25],

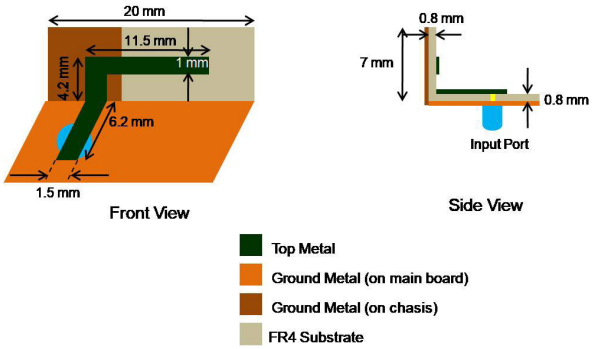


**FIGURE 12.** Schematic of the single element of 4-port MIMO antenna system.

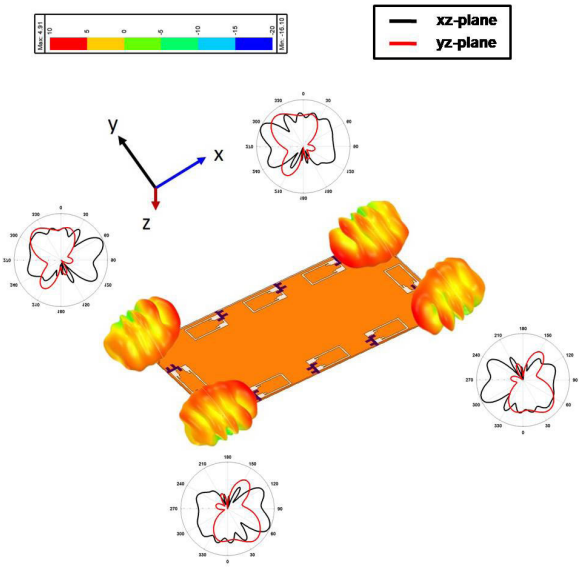


**FIGURE 13.** Radiation patterns of individual antenna elements of the proposed 4-port MIMO antenna.

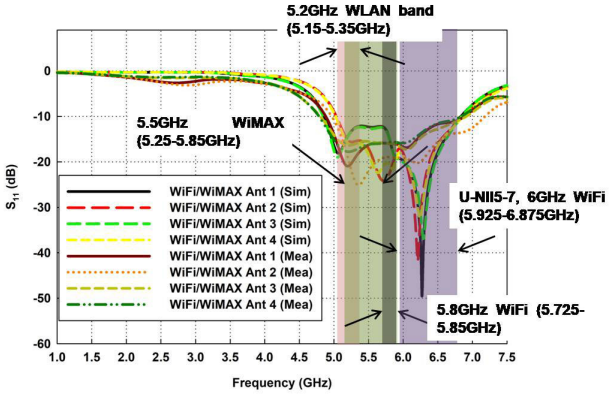


**FIGURE 14.** Individual S-parameters for all the antenna elements of 4-port MIMO antenna system.

5.5 GHz WiMAX band (5.25 GHz to 5.85 GHz), 5.8 GHz WiFi band (5.725 GHz to 5.825 GHz) [26] and three channels U-NII 5 (5.925 GHz to 6.425 GHz), U-NII 6 (6.425 GHz

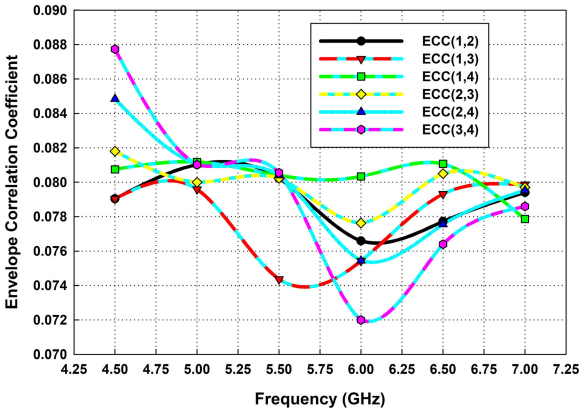


**FIGURE 15.** Envelope correlation coefficient associated with 4-port MIMO antenna.

**TABLE 1.** Comparison of the proposed dual MIMO antenna system with current state of the art.

| Ref. No. | Frequency Range | Isolation | ECC | No. of Elements |
|---|---|---|---|---|
| [28] | 2.4-3.6 GHz | >15 dB | <0.2 | 8 |
| [29] | 3.25-3.82 GHz; 4.79-6.2 GHz | >10.5 dB | <0.12 | 8 |
| [30] | 3.4-3.6 GHz | >13 dB | <0.27 | 6 |
| [31] | 3.3-7.5 GHz | >10 dB | <0.06 | 4 |
| [32] | 3.3-5.6 GHz | >15 dB | <0.03 | 8 |
| [33] | 3.3-4.2 GHz | >10.5 dB | <0.2 | 8 |
| [34] | 3.3-5 GHz | >12 dB | <0.11 | 8 |
| **This work** | **3.37-3.6 GHz; 5.02-6.93 GHz** | **>19.5 dB** | **<0.08** | **8+4** |

to 6.525 GHz) and U-NII 7 (6.525 GHz to 6.875 GHz) designated for very promising WiFi 6E band [27]. The ECCs associated with this MIMO are computed using (1) and is shown in Fig. 15. For the frequency range 4.5 GHz to 7 GHz, covering all of the aforementioned bands, it can be seen that the ECC complies with the accepted limits.

### C. SPECIFIC ABSORPTION RATE (SAR)

Specific Absorption Rate (SAR) estimates the rate at which the RF energy from the device under test is absorbed by the body [29]. Standard SAR value for cell phones is 1.6 W/kg for 1g tissue. Fig. 16a shows the SAR distribution for 8-port MIMO antenna at 3.5 GHz. All of the ports were fed with equal input power. The sum of the input powers from all of the ports was 100 mW (20dBm). The SAR distribution was obtained for 1g tissue. It can be seen the maximum value of SAR for 8-port MIMO antenna is 0.49 W/kg. Fig. 16b shows the SAR distribution for 4-port MIMO antenna at 5.5 GHz. Input power of 100 mW was equally divided among the four ports to obtain the SAR distribution. It can be seen that the maximum value of SAR for the 4-port MIMO antenna is 1.33 W/kg for 1g tissue, which is well within acceptable limits.

### D. COMPARISON AND DISCUSSION

The performance of the proposed dual MIMO antenna system is analyzed and depicted with respect to the state of art

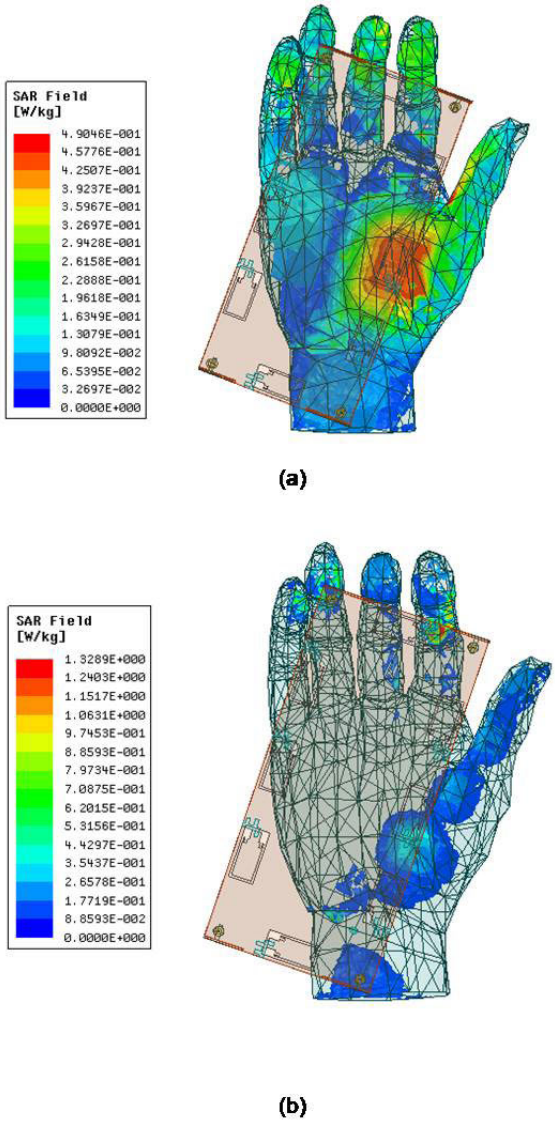


**FIGURE 16.** SAR distribution of the proposed dual MIMO antenna system (a) SAR for 8-port MIMO antenna at 3.5 GHz (b) SAR for 4-port MIMO antenna at 5.5 GHz.

in Table 1. As can be seen, the isolation between individual antenna elements is more agreeable than many of the recent designs. The ECC between the radiators is also very agreeable according to accepted standards.

## III. CONCLUSION

This paper presents a dual MIMO antenna system for 5G mobile phones. The prototype consists of a 8-port MIMO antenna and a 4-port MIMO antenna operating on two separate bands. The main merit of the proposed antenna system is that it covers five relevant frequency bands. The 8-port MIMO antenna operates at 3.5 GHz allocated for 5G applications in the sub-6 GHz spectrum. 4-port multiband MIMO antenna operates at 5.2 GHz WLAN, 5.5 GHz WiMAX, 5.8 GHz WiFi bands and channels U-NII5-7 for much

anticipated 6 GHz WiFi applications. All antenna elements are well isolated with the nearby radiators. Measurements with the fabricated prototype and simulation demonstrate relatively good agreement, indicating that it is suitable in mobile devices for upcoming 5G systems.

## REFERENCES

[1] R.-L. Haupt, *Wireless Communications Systems: An Introduction*. Hoboken, NJ, USA: Wiley, 2020, pp. 1–15.

[2] D. T. Emerson, "The work of jagadis chandra bose: 100 years of millimeter-wave research," *IEEE Trans. Microw. Theory Techn.*, vol. 45, no. 12, pp. 2267–2273, Dec. 1997, doi: 10.1109/22.643830.

[3] X. Ma, F. Yang, S. Liu, J. Song, and Z. Han, "Design and optimization on training sequence for mmWave communications: A new approach for sparse channel estimation in massive MIMO," *IEEE J. Sel. Areas Commun.*, vol. 35, no. 7, pp. 1486–1497, Jul. 2017, doi: 10.1109/JSAC.2017.2698978.

[4] J. Winters, "Optimum combining for indoor radio systems with multiple users," *IEEE Trans. Commun.*, vol. I-35, no. 11, pp. 1222–1230, Nov. 1987, doi: 10.1109/TCOM.1987.1096697.

[5] E. Björnson, L. Sanguinetti, H. Wymeersch, J. Hoydis, and T. L. Marzetta, "Massive MIMO is a reality—What is next?: Five promising research directions for antenna arrays," *Digit. Signal Process.*, vol. 94, pp. 3–20, Nov. 2019, doi: 10.1016/j.dsp.2019.06.007.

[6] B. H. Khalaj, A. Paulraj, and T. Kailath, "Antenna arrays for CDMA systems with multipath," in *Proc. IEEE Mil. Commun. Conf. (MILCOM)*, Boston, MA, USA, Oct. 1993, pp. 624–628, doi: 10.1109/MILCOM.1993.408593.

[7] G. J. Foschini, "Layered space-time architecture for wireless communication in a fading environment when using multi-element antennas," *Bell Labs Tech. J.*, vol. 1, no. 2, pp. 41–59, Feb. 1996, doi: 10.1002/bltj.2015.

[8] M. A. Jensen, "A history of MIMO wireless communications," in *Proc. IEEE Int. Symp. Antennas Propag. (APSURSI)*, Fajardo, PR, USA, Jun. 2016, pp. 681–682, doi: 10.1109/APS.2016.7696049.

[9] R. Ullah, S. Ullah, R. Ullah, F. Faisal, I. B. Mabrouk, and M. J. A. Hasan, "A 10-ports MIMO antenna system for 5G smartphone applications," *IEEE Access*, vol. 8, pp. 218477–218488, Dec. 2020, doi: 10.1109/ACCESS.2020.3042750.

[10] S. K. Goudos, P. D. Diamantoulakis, and G. K. Karagiannidis, "Multiobjective optimization in 5G wireless networks with massive MIMO," *IEEE Commun. Lett.*, vol. 22, no. 11, pp. 2346–2349, Nov. 2018, doi: 10.1109/LCOMM.2018.2868663.

[11] M. Ikram, E. A. Abbas, N. Nguyen-Trong, K. H. Sayidmarie, and A. Abbosh, "Integrated frequency-reconfigurable slot antenna and connected slot antenna array for 4G and 5G mobile handsets," *IEEE Trans. Antennas Propag.*, vol. 67, no. 12, pp. 7225–7233, Dec. 2019, doi: 10.1109/TAP.2019.2930119.

[12] H. A. Diawuo and Y.-B. Jung, "Broadband proximity-coupled microstrip planar antenna array for 5G cellular applications," *IEEE Antennas Wireless Propag. Lett.*, vol. 17, no. 7, pp. 1286–1290, Jul. 2018, doi: 10.1109/LAWP.2018.2842242.

[13] I. Syrytsin, S. Zhang, G. F. Pedersen, and Z. Ying, "User effects on the circular polarization of 5G mobile terminal antennas," *IEEE Trans. Antennas Propag.*, vol. 66, no. 9, pp. 4906–4911, Sep. 2018, doi: 10.1109/TAP.2018.2851383.

[14] C. Di Paola, K. Zhao, S. Zhang, and G. F. Pedersen, "SIW multibeam antenna array at 30 GHz for 5G mobile devices," *IEEE Access*, vol. 7, pp. 73157–73164, 2019, doi: 10.1109/ACCESS.2019.2919579.

[15] M. Ikram, N. N. Trong, and A. Abbosh, "Hybrid antenna using open-ended slot for integrated 4G/5G mobile application," *IEEE Antennas Wireless Propag. Lett.*, vol. 19, no. 4, pp. 710–714, Apr. 2020, doi: 10.1109/LAWP.2020.2978181.

[16] J. Liu and B. Zhang, "A modularized interchangeable multibeam slot array antenna using hybrid substrates for mass production," *IEEE Antennas Wireless Propag. Lett.*, vol. 20, no. 5, pp. 723–727, May 2021, doi: 10.1109/LAWP.2021.3061427.

[17] D. Huang, Z. Du, and Y. Wang, "A quad-antenna system for 4G/5G/GPS metal frame mobile phones," *IEEE Antennas Wireless Propag. Lett.*, vol. 18, no. 8, pp. 1586–1590, Aug. 2019, doi: 10.1109/LAWP.2019.2924322.

[18] Z. Ren, A. Zhao, and S. Wu, "MIMO antenna with compact decoupled antenna pairs for 5G mobile terminals," *IEEE Antennas Wireless Propag. Lett.*, vol. 18, no. 7, pp. 1367–1371, Jul. 2019, doi: 10.1109/LAWP.2019.2916738.

[19] Z. Xu and C. Deng, "High-isolated MIMO antenna design based on pattern diversity for 5G mobile terminals," *IEEE Antennas Wireless Propag. Lett.*, vol. 19, no. 3, pp. 467–471, Mar. 2020, doi: 10.1109/LAWP.2020.2966734.

[20] K. L. Wong, J. Y. Lu, L. Y. Chen, W. Y. Li, and Y. L. Ban, "8-antenna and 16-antenna arrays using the quad-antenna linear array as a building block for the 3.5-GHz LTE MIMO operation in the smartphone," *Microw. Opt. Technol. Lett.*, vol. 58, no. 1, pp. 174–181, Jan. 2016, doi: 10.1002/mop.29527.

[21] P. Mathur, G. Madanan, and S. Raman, "Mechanically frequency reconfigurable antenna for WSN, WLAN, and LTE 2500 based Internet of Things applications," *Int. J. RF Microw. Comput.-Aided Eng.*, vol. 31, no. 2, Feb. 2021, Art. no. e22318, doi: 10.1002/mmce.22318.

[22] Arista. *6 GHz WiFi–The Silver Bullet for Addressing the 1000X Data Challenge Using Unlicensed Spectrum*. Accessed: Jun. 26, 2020. [Online]. Available: https://www.arista.com/assets/data/pdf/Whitepapers/Arista-6GHz-WiFi-WP.pdf

[23] A. Narbudowicz, M. J. Ammann, and D. Heberling, "Impact of lossy feed on S-parameter based envelope correlation coefficient," in *Proc. 10th Eur. Conf. Antennas Propag. (EuCAP)*, Davos, Switzerland, Apr. 2016, pp. 1–3, doi: 10.1109/EuCAP.2016.7481596.

[24] R. Cornelius, A. Narbudowicz, M. J. Ammann, and D. Heberling, "Calculating the envelope correlation coefficient directly from spherical modes spectrum," in *Proc. 11th Eur. Conf. Antennas Propag. (EUCAP)*, Paris, France, Mar. 2017, pp. 3003–3006, doi: 10.23919/EuCAP.2017.7928132.

[25] L. Guo, Y. Wang, Z. Du, Y. Gao, and D. Shi, "A compact uniplanar printed dual-antenna operating at the 2.4/5.2/5.8 GHz WLAN bands for laptop computers," *IEEE Antennas Wireless Propag.*, vol. 13, pp. 229–232, 2014, doi: 10.1109/LAWP.2014.2303495.

[26] A. A. Talukder, D. K. Karmokar, K. M. Morshed, and M. N. Mollah, "Low profile inverted-FL antenna for 5.5 GHz WiMAX applications," *ACEEE Int. J. Commun.*, vol. 3, no. 1, pp. 15–19, Mar. 2012.

[27] A. Pai, M. O'Rielly, B. Carr, J. Rosenworcel, and G. Starks, "Unlicensed use of the 6 GHz band, expanding flexible use in mid-band spectrum between 3.7 GHz and 24 GHz," Federal Commun. Commission, Washington, DC, USA, ET Docket No. 18-295, and GN Docket No. 17-183, Apr. 2020. [Online]. Available: https://docs.fcc.gov/public/attachments/FCC-20-51A1.pdf

[28] M. Abdullah, S. H. Kiani, and A. Iqbal, "Eight element multiple-input multiple-output (MIMO) antenna for 5G mobile applications," *IEEE Access*, vol. 7, pp. 134488–134495, 2019, doi: 10.1109/ACCESS.2019.2941908.

[29] H. Wang, R. Zhang, Y. Luo, and G. Yang, "Compact eight-element antenna array for triple-band MIMO operation in 5G mobile terminals," *IEEE Access*, vol. 8, pp. 19433–19449, Jan. 2020, doi: 10.1109/ACCESS.2020.2967651.

[30] M. Abdullah, S. H. Kiani, L. F. Abdulrazak, A. Iqbal, M. A. Bashir, S. Khan, and S. Kim, "High-performance multiple-input multiple-output antenna system for 5G mobile terminals," *Electronics*, vol. 8, no. 10, p. 1090, Sep. 2019, doi: 10.3390/electronics8101090.

[31] X.-T. Yuan, Z. Chen, T. Gu, and T. Yuan, "A wideband PIFA-pair-based MIMO antenna for 5G smartphones," *IEEE Antennas Wireless Propag. Lett.*, vol. 20, no. 3, pp. 371–375, Mar. 2021, doi: 10.1109/LAWP.2021.3050337.

[32] Z. Yu, M. Wang, and Y. Xie, "An improved loop ultra-wideband MIMO antenna SYSTEM for 5G mobile terminals," *Prog. Electromagn. Res. Lett.*, vol. 93, pp. 99–106, 2020.

[33] L. Sun, Y. Li, Z. Zhang, and H. Wang, "Self-decoupled MIMO antenna pair with shared radiator for 5G smartphones," *IEEE Trans. Antennas Propag.*, vol. 68, no. 5, pp. 3423–3432, May 2020, doi: 10.1109/TAP.2019.2963664.

[34] L. Sun, Y. Li, Z. Zhang, and Z. Feng, "Wideband 5G MIMO antenna with integrated orthogonal-mode dual-antenna pairs for metal-rimmed smartphones," *IEEE Trans. Antennas Propag.*, vol. 68, no. 4, pp. 2494–2503, Apr. 2020, doi: 10.1109/TAP.2019.2948707.

**PHALGUNI MATHUR** (Student Member, IEEE) received the B.Sc. degree (Hons.) in physics from the University of Delhi, in 2012, and the M.Sc. degree in electronics from Cochin University of Science and Technology (CUSAT), Cochin, Kerala, India, in 2015. She is currently pursuing the Ph.D. degree with the Department of Electronics and Instrumentation, Bharathiar University, Coimbatore, Tamil Nadu, India. Her doctoral research is focused mainly in the area of reconfigurable antenna systems for 5G MIMO and the Internet of Things (IoT) systems. She has previous research experience in the field of radomes, RCS reduction for stealth systems, and radio astronomy. Some other areas of research that she is currently working on are RFID systems, RF circuits, and computational electromagnetics, among others. She received the Young Scientist Award at URSI-GASS-2021, Rome, Italy.

**ROBIN AUGUSTINE** (Member, IEEE) received the bachelor's degree in electronics science from Mahatma Gandhi University, Kottayam, India, in 2003, the master's degree in robotics from Cochin University of Science and Technology, Cochin, India, in 2005, and the Ph.D. degree in electronics and optronics systems from the Universite de Paris Est Marne La Vallee, France, in 2009. He completed his postdoctoral training at IETR, University of Rennes 1, from 2009 to 2011. Since 2011, he has been a Senior Researcher with Uppsala University, Sweden. In 2016, he was appointed as a Docent (Associate Professor) in microwave technology with Uppsala University. He is currently an Associate Professor in medical engineering and is leading the Microwaves in Medical Engineering Group (MMG), Solid State Electronics Division, Uppsala University. Since 2019, he has been a Visiting Professor with Beijing Institute of Nanoenergy and Nanosystems (BINN), Beijing. He is the Swedish P.I. of the Eureka Eurostars Project COMFORT, MAS, and Indo-Swedish Vinnova-DST funded project BDAS. He was granted the Swedish Research Council (V.R.) funding for his project Osteodiagnosis. He is also the W.P. Leader of the H2020 Project SINTEC and a Co-PI of the framework project LifeSec and Zero-IoT from the Swedish Strategic Foundation (SSF). He is responsible for the lead technical development in the Eurostars Project SenseBurn. He is coordinating the H2020 FET Open Project B-CRATOS on brain–machine interface. He is the author or coauthor of more than 170 publications, including journals and conferences in the field of sensors, microwave antennas, electrophysiology, intrabody communication, microwave phantoms, bio-electromagnetics, and material characterization. He holds three patents in the field of musculoskeletal sensing using microwaves. His current research interests include the design of wearable antennas, BMD sensors, dielectric characterization, intrabody area networks, bio electromagnetism, non-invasive diagnostics, bionics, brain–computer interface, fat-intrabody communication, and biomechatronic. He is a member of the Editorial Board for the *Electronics Letters* (IET). He was a recipient of the Maroun Seeman Fellowship awarded by AUB, Beirut, Lebanon. He has received twice the Attractive Innovative Prize from Uppsala University Innovation, in 2020. He received the UGCRFSMS Fellowship for meritorious students from the Government of India and the EGIDE Eiffel Grant for excellence from the French Research Ministry, in 2006 and 2008, respectively.

**M. GOPIKRISHNA** (Member, IEEE) received the M.Sc. degree from the Department of Physics, Cochin University of Science and Technology (CUSAT), Kerala, India, in 2001, and the Ph.D. degree in microwave electronics from the Department of Electronics, CUSAT, in 2010. He is currently with the Department of Collegiate Education, Government of Kerala, India, as an Assistant Professor of physics. His research has mostly been in developing planar printed antennas for ultra-wide band (UWB) systems in which he has published several papers in international journals and conferences. He has monographed two books and has contributed to a book chapter in IntechOpen. His current research interests include metamaterials, CRLH-TL, microwave filters, UWB/MIMO antennas, and microwave sensors. He is a reviewer to papers in a few leading international journals.

**SUJITH RAMAN** (Senior Member, IEEE) was born in India. He received the B.Sc. degree in physics from the Government Victoria College, Palakkad, and the University of Calicut, India, in 2003, the bachelor's degree in education from University Teacher Education Centre, Palakkad, and the University of Calicut, in 2005, and the M.Sc. degree in electronic science and the Ph.D. degree in microwave electronics from Cochin University of Science and Technology (CUSAT), India, in 2007 and 2012, respectively. In March 2016, he joined Bharathiar University, as a Faculty. He was with the Solid State Electronics, Angstrom Laboratory, Uppsala University, Sweden, as a Postdoctoral Researcher. He was with the WiSAR Lab, Letterkenny Institute of Technology, Ireland, as a Postdoctoral Researcher. He is currently working as an UGC-Assistant Professor at Bharathiar University, India. He is the author or coauthor of more than 60 publications, including journals and conferences. His research interests include the designing of antennas, planar microwave devices, bioelectromagnetics, and microwave material characterization. He is a Senior Member of URSI. He received the URSI Young Scientist Award at URSIGASS 2011, Istanbul, Turkey, and URSI–RCRS-2017 at Tirupati, India.